Available online at www.sciencedirect.com

ScienceDirect

Energy Procedia 129 (2017) 403–410

Energy Procedia

www.elsevier.com/locate/procedia

IV International Seminar on ORC Power Systems, ORC2017
13-15 September 2017, Milano, Italy

Experimental and Numerical Characterization of an Oil-Free Scroll Expander

Alessio Suman*[,a], Saverio Randi[a], Nicola Casari[a], Michele Pinelli[a], Luca Nespoli[b]

[a] *Engineering Department in Ferrara (EnDiF), University of Ferrara, Ferrara, Italy*
[b] *Energeticamente Rinnovabili srl, Torino, Ferrara, Italy*

Abstract

Micro-ORC systems are characterized by low efficiency values, but at the same time could be used as energy recovery systems in domestic applications for which reliability and low noise level represent the biggest challenges. In this paper, an integrated Reverse Engineering (RE)-Computational Fluid Dynamics (CFD) methodology is applied in order to study the adaptation of a commercial scroll compressor to be used as an expander in a micro-ORC system.
The analyses reported in this paper consist of: (i) the acquisition of the 5-kW oil-free scroll expander through a RE procedure and its CAD reconstruction, (ii) the set-up of fully three-dimensional transient simulations with the Chimera strategy using the Siemens PLM software, (iii) the validation of the computational analysis by means of experimental tests and finally, (iv) the analysis of the geometry-flow features like flank and axial gaps, coupled with the analysis of the scroll volumetric efficiency and overall performance. Chimera strategy is able to move the computational grid at each time step in order to accommodate the shape and size changes of the gas pockets.
The scroll characterization was carried out using both experimental and numerical tests. Six different rotational velocities in the range of (400 – 2400) rpm with a fixed pressure level (7.5 bar) were tested for validating the numerical model using air as a working fluid. The numerical model was then used to calculate the scroll expander performance operating in an existing ORC system with R134a as working fluid.

Peer-review under responsibility of the scientific committee of the IV International Seminar on ORC Power Systems.

Keywords: scroll expander; computational fluid dynamics, moving mesh, Chimera strategy; experimental validation

* Corresponding author. Tel.: +39-0532-974964;
E-mail address: alessio.suman@unife.it

1876-6102
Peer-review under responsibility of the scientific committee of the IV International Seminar on ORC Power Systems.
10.1016/j.egypro.2017.09.120

Nomenclature

T	torque	peak	peak value
n	rotational velocity	CFD	Computational Fluid Dynamics
V	volume flow rate	FS	Full Scale
y^+	dimensionless distance	RE	Reverse Engineering
Z	compressibility factor	DAQ	Data AcQuisition device

1. Introduction

In the last decade, several studies related to micro-ORC applications were reported [1]. Many of these, (up to 10 kW) use a scroll as expander [2] thanks to its reliability, compact structure, relative few moving parts and low level of noise. Examples of these applications, having an average value of scroll power equal to 2 kW, can be found in [3 – 5]. In [3] an open-drive oil-free air scroll compressor with a 4.05 built-in volume ratio was investigated, while in [4] an hermetic scroll compressor design for heat pump applications with a 3.00 built-in volume ratio was used. Eventually, the analysis concerning an air scroll compressor with a 3.95 built-in volume ratio is reported in [5]. Moving to lower power range, approximately equal to 1 kW, in [6] a semi-custom, commercially derived scroll expander with a 2.5 expansion ratio was used. Other applications are reported in [7], where an in-house designed scroll compressor was analysed, and in [8] in which a modified hermetic scroll compressor was studied.

The performances of the volumetric expander are related, in particular, to the variation of the isolated volumes during rotation and the seals. Indeed, understanding the relationship between the scroll spiral profiles and, therefore, scroll pockets evolution and the machine overall performances both in terms of energy and mechanics is the first step towards understanding scroll machine working behavior. For these reasons, laboratory micro- and sub-systems have been developed in order to study and optimize the scroll geometry. At the same time, CFD numerical analyses have been carried out in order to discover flow peculiarities that could affect the overall scroll performance.

Numerical simulation for the scroll machine is still in an early stage because of the complex geometry and unique motion of orbiting scroll wrap [9]. Particularly, the interaction between moving part and the fixed one represent the great challenge in this application. The CFD model allows for the evaluation of the influence of leakage flows, e.g. due to radial (flank) gaps, which play a key role in the determination of the performances of the machine, as for instance, cavitation phenomena [10] or pressure fluctuation [11]. Moreover, it can be used for the tuning of analytical and thermodynamic models with fewer resources in the design phase [12].

In the present paper, the actual geometry of a commercial available oil-free scroll air compressor has been acquired by means of a RE procedure in order to perform a CFD analysis. This procedure represents a very useful method for generating a computational geometry of the real machine, and in the last years its reliability has increased dramatically. Instrumentation and methodology have improved their accuracy and, at the same time, the progress in software development allows three-dimensional representation of real objects in a very short time [13, 14].

The consequent CFD analysis was conducted using a Chimera strategy that is proven to give comparable results with other transient numerical simulation based on moving mesh [15] on a fully three-dimensional scroll geometry. At the preliminary stage, the validity of the computational strategy was checked comparing numerical results with the experimental one. The experimental procedure was conducted on the scroll expander using air as a working fluid. Subsequently, the scroll expander performance was calculated using the R134a and a detailed flow field analysis was conducted.

In synthesis, the main contributions of this paper are:

- the application to a real world scroll machine of a combined RE/CFD methodology which allowed to gather information regards flank gaps, actual geometric features of scroll profile nose. These details seldom are available either in literature or from manufacturer data;
- the utilization of the Chimera approach for the analysis, made it possible to investigate the fluid dynamics of small and variable-with-orbit flank gaps. This feature is usually modelled as if the gap size is fixed and by using values greater than 100 μm;
- the evaluation of scroll performance operating with R134a in an actual ORC system.

2. Chimera strategy

In the present paper, the CFD analysis has been conducted using the Chimera strategy as mesh adaption technique. Chimera strategy, known also with the name of overlapping grid or overset method, was first introduced in the early 1980's [16] when several grid assembly packages have become available [17]. In the present paper, the simulations of the scroll expander were carried out by means of Siemens PLM software 11.02.

Chimera strategy usually involves one background mesh, which is adapted to environment, and one or more overset grids attached to bodies, overlapping the background mesh and/or each other as reported in Fig. 1a, adopted from [18]. Each grid can move according to the motion models implemented in the CFD software. The peculiarity of this type of approach is related to the complete absence of mesh deformation during the transient calculation. An overset mesh consists in the contemporary use of active and passive cells. In active cells, regular discretized equations are solved, while in passive cells, no equation is solved, they are temporarily or permanently de-activated. Since the solution is computed on all grids simultaneously, to link the results in the background region to the ones obtained in overset regions, acceptor and donor cells are used; acceptor cells represent the very first layer of passive cells near active ones and exchange data with donor cells, which belong to the other mesh and have to be active cells: the change of cell status is automatically controlled by the solver. Grids are implicitly coupled through the linear equation system matrix. Different interpolation functions can be used to express values at acceptor cells via values at donor cells. Figure 1b depicts a sketch of the flank gap, also visible in Fig. 2 together with the background mesh and the overlapping mesh. The overlapping mesh bounds the moving scroll spiral and was obtained by an offset of 1 mm from the actual moving scroll spiral.

The Overlapping mesh employed in this work is made up of about 7 million elements while the background mesh (that refers to the scroll stator and fixed spiral) is made up by about 12 million elements. Both overlapping and background meshes are composed by polyhedral elements and prism layers close to the wall as showed in Fig. 2, where are clearly visible the polyhedral elements in the core regions and the prism layers near the domain boundaries. Prims layers allow the grid refinement and the good representation of the scroll flank leakage.

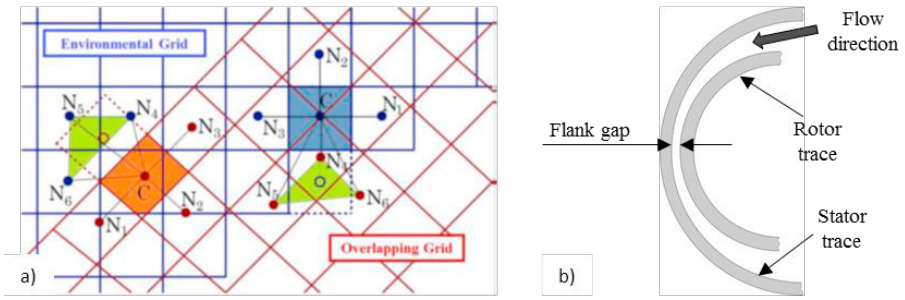

Fig. 1. a) N1, N2, N3 neighbors from same grid; N4, N5, N6 neighbors from overlapping grid [18] and b) sketch of the flank gap

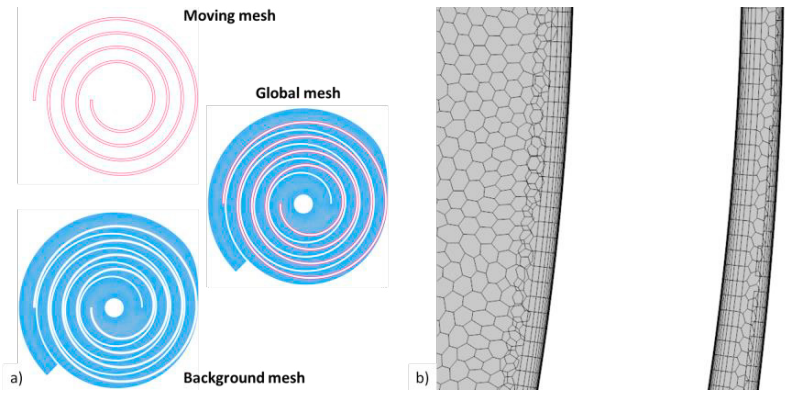

Fig. 2. Chimera strategy applied to a scroll: a) background and moving meshes and b) detail of the mesh in narrow gaps

3. Numerical setup and experimental validation

As mentioned above, this paper deals with the numerical simulation of a commercial available oil-free scroll air compressor converted as an expander. Figure 3 reports the actual scroll and the virtual model obtained after RE procedure by means of a three-dimensional solid modeler. Table 1 summarizes the geometric characteristics and performance of the scroll working as a compressor; the reader should notice that the flank gap is variable over the orbit up to 300 μm. This is related to the scroll typology: oil-free design has to guarantee a minimum distance between the moving and fixed spirals avoiding the mutual friction. This non-fixed gap is one of the challenging aspects of scroll machine modeling together with the variable-with-crankshaft angle volume of the gas pockets; thus, extra care should be taken when setting up the numerical simulation and carrying out the CFD analysis.

3.1. Boundary conditions

For the simulations of scroll expander using air as working fluid, the results were validated against experimental data for an inlet pressure of 7.5 bar and six different rotating speeds: 400 rpm, 800 rpm, 1200 rpm, 1600 rpm, 2000 rpm and 2400 rpm. The numerical model was set up as follows: a stagnation inlet boundary condition was imposed on a circle centered in the middle of the stator trace, with 7.5 bar as inlet pressure and 292 K as inlet temperature, while a pressure value equal to 1.013 bar was imposed at the physical output of the scroll machine. Stator and rotor surfaces were considered as adiabatic walls, while the 1 mm-extruded overset surface was set as an overset mesh interface, which defines moving and stationary domains.

With regards to turbulence modeling, the realizable k-ε model with a two-layer y^+ wall treatment was chosen, in order to model the flow across the gaps with a higher accuracy than the one offered by the realizable k-ε model with standard wall functions. In fact, realizable model is predicted to give better results than the standard model for flows involving rotation and strong streamline curvature [19], as the one which can be encountered inside a scroll machine, while the two-layer approach has been chosen because of the different y^+ values for the first cell inside the flank gap and the first cell outside this gap.

Air was modeled as a real gas using the Redlich-Kwong equation of state, to consider the effective behavior of the gas even if only the third decimal place of Z varies, under the actual operating conditions of the expander. This choice was taken in order to create a simulation template useful for the future comparison of the performance of scroll machines under the same operating conditions, except for the working fluid.

The hybrid mesh approach (polyhedral cells in the core domain and prismatic cell type near the boundaries) adopted in this work could reduce the stability of the solution related to the numerical scheme, together with the

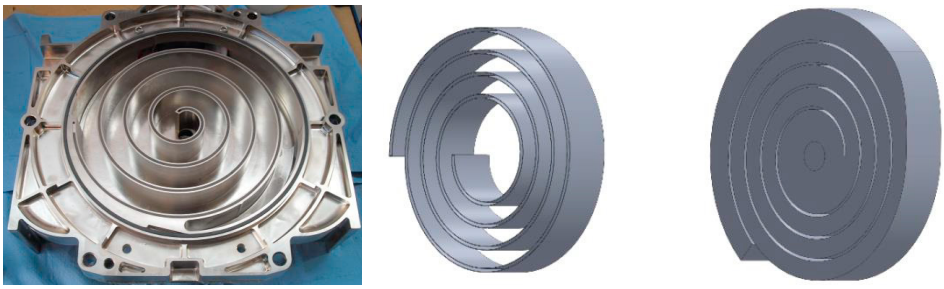

Fig. 3. Oil-free scroll air compressor: internal view and solid modeler reconstruction

Nominal power	5 kW
Volume ratio	3.5
Displacement	73,000 mm^3/rev
Maximum rotational velocity	2600 rpm
Flank gaps	20 – 300 μm

Table 1. Oil-free scroll air compressor geometric characteristics and performance

contemporary presence of stretched meshes (for more details see [20]). For these reasons, great care has been taken in the choice of temporal discretisation. The CFD analyses have been carried out with a variable time step, ranging from 1e-5 s to 5e-6 s depending on the scroll rotational speed and initialized with a solution obtained with a first order Upwind advection scheme, before passing to the second order one. The simulation with R134a as working fluid was set up with the same conditions listed above apart from the time step, diminished to 1e-6 s.

3.2. Pressure and velocity fields for the air-driven scroll

Solution of the pressure field inside the machine is presented in Fig. 4 as a function of the normalized angular position of the rotor with respect to the stator. A comparison between the results obtained for 800 rpm and 2400 rpm velocities is shown. These results are similar to the ones reported in [21], comparing the zones of the machine with the highest and lowest pressures. In fact, it is possible to see that, due to the machine geometry, pressure values at the suction chamber are constant during the whole expansion process, while they slowly decrease in the other chambers along with crankshaft rotation.

Velocity values inside the machine are of great importance, because high values can be encountered in axial and radial gaps and thus they can lead to energy dissipation related to eddies structure. Furthermore, this is emphasized in oil-free expanders, where gaps are wider than lubricated machine ones. In the current geometry, is visible how velocity magnitude is greater in the gaps and in the outlet duct (vectors with the biggest tip) as reported in Fig. 5.

3.3. Scroll test bench

The experimental data presented in this paper were collected by means of a test bench equipped with several

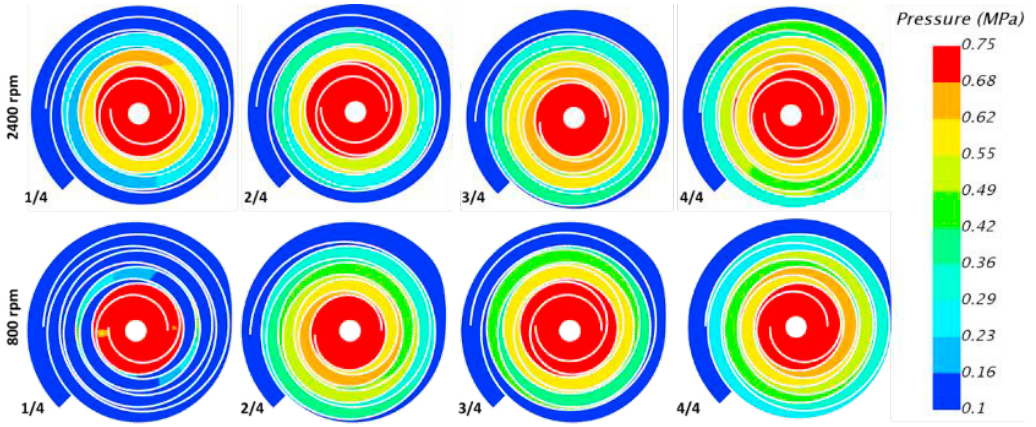

Fig. 4. Pressure plots on a section plane perpendicular to machine axis.

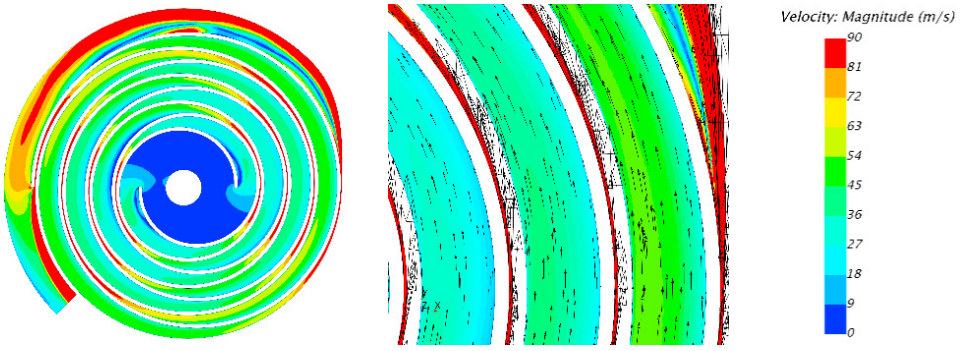

Fig. 5. Global velocity magnitude of the fluid and flank leakages (2000 rpm)

sensors: pressure transducers, flowmeter, load cell, rotational speed sensor and temperature probes. The pressure transducers for the inlet and outlet pressure measurements were thin-film sensors with 16 bar FS and ± 0.5 % FS accuracy: the first was placed 1.5 m before the scroll inlet port, while the second was screwed downstream the plenum used to damp pressure fluctuations. The flow meter was placed upstream the inlet pressure sensor and it was a thermal type one with 0.05 m^3/s FS and ± 1.8 % FS accuracy. The load cell (10 kg FS with ± 0.05 % FS accuracy) was placed between the expander and the electrodynamic brake. The rotational speed sensor was a Hall-effect one, which measures the velocity with a resolution of one sample per scroll shaft revolution. Temperature probes, A-class Pt100 probe, for the flow at the inlet and outlet of the machine, were positioned near pressure transducers.

Data was acquired by means of a DAQ which introduced a maximum accuracy of ± 1 K for temperature and less than ± 1 % of reading for the other analog current signals. The A/B-type uncertainty of 2.5 % of reading was estimated, to take into account others contribution to uncertainty which were not, a priori, known (such as installation, flow conditions, etc.).

3.4. Data comparison

Experimental results reported in Fig. 6 are referred to average values obtained during stationary working condition of the scroll expander. The trends depicted in Fig. 6 show that the CFD results are similar to the measured ones, even if the former are always greater than the on-site values. This is due to the fact that the gaps of the numerical model are wider than the real ones, because of numerical issues given by mesh updating process. In light of this, wider gaps cause an increase in fluid leakages, with a decrease of pressure in first expander chambers and an increase in the last ones, allowing for a higher torque and an augmented fluid flow at the inlet with respect to the effective geometry. Both of these aspects are visible in the graphs of Fig. 6; no error bars are shown because of the small magnitude of the uncertainties, less than 0.0013 m^3/s and 0.10 Nm. On the other hand, trend showed by CFD results is very similar to the experimental one as reported in Fig. 7, where data are presented in dimensionless form, obtained by dividing each result for the peak value.

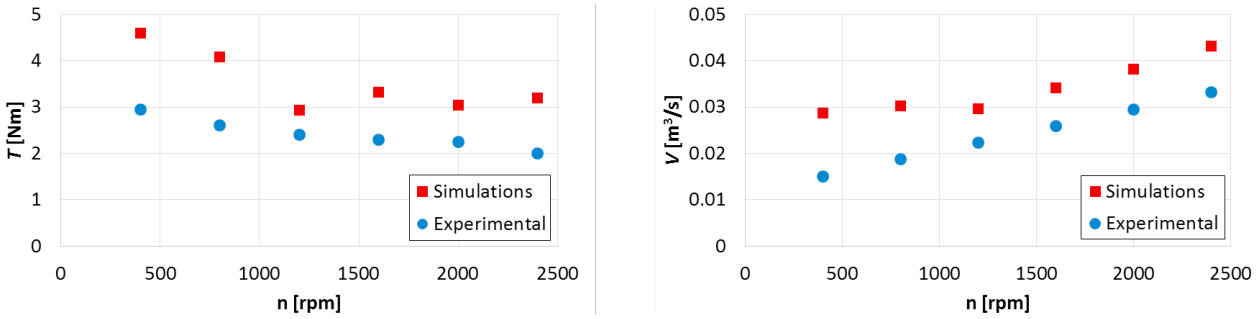

Fig. 6. Numerical versus experimental results: torque and volume flow at the inlet section

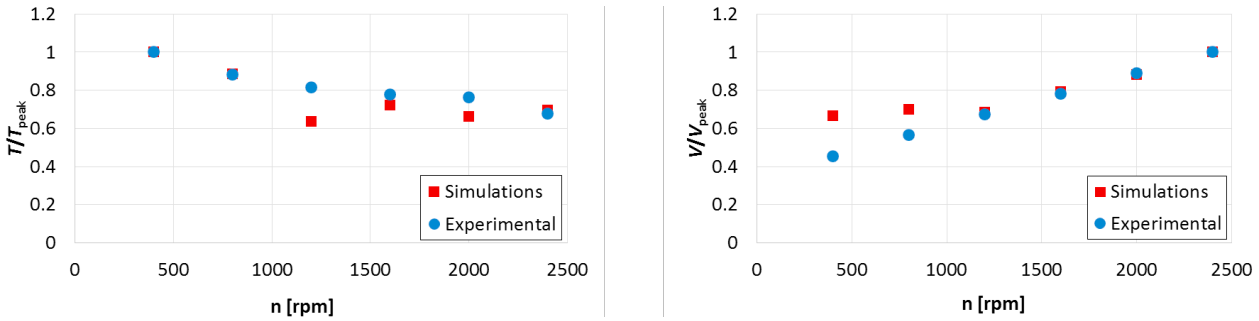

Fig. 7. Numerical versus experimental results: dimensionless values of torque and volume flow at the inlet section

4. Scroll operation in an actual ORC system

After model validation, a simulation was run in order to assess the behaviour of the scroll machine employed as the expander of an off-the-shelf ORC system described in [22]. In this study, 1,1,1,2-tetrafluoroethane (R134a) was chosen as the working fluid. The pressure at the inlet section of the expander was set equal to 13.9 bar while the inlet temperature of the fluid was 338 K. At the outlet port the value of 296 K was imposed. To match the scroll expander volume ratio (see Table 1), the rotational speed imposed for the CFD analysis is equal to about 350 rpm.

4.1. Results analysis

Figure 8 shows the output torque and the volume flow rate at the inlet as functions of the normalized crankshaft angle. Their average values are 4.3 Nm and 0.011 m^3/s. It is possible to see the great variation of torque values, ranging from 1.3 Nm to 8.5 Nm, which can lead to vibrations of the expansion device during the actual operation. In Fig. 9 are then showed plots of the pressure inside the expander; pressure distribution is similar to the one found when studying the expander behavior with air as working fluid. Cases with similar pressure distribution inside the expander chambers can be found in literature [2, 9, 15].

5. Conclusions

In this paper, the CFD study of a scroll expander and its validation against real data has been presented. The actual operation of the scroll expander was modeled by means of overset mesh coupled with transient analyses with real gas models. Data regarding pressure and velocity field inside the expander, torque and volume flow rate at the inlet are shown. The numerical model, which was validated against experimental data, was able to capture torque and mass flow rate trends, while a certain deviation (up to 100 % in volume flow rate values) is highlighted, due to the higher values of flank gaps which cause a large amount of fluid to leak. Using the CFD model, the application of a specific scroll expander geometry to an existing ORC system was carried out. Results related to torque and flow rate trends are useful to discover the possibility to improve the analysis of this device, and more in general, to detect

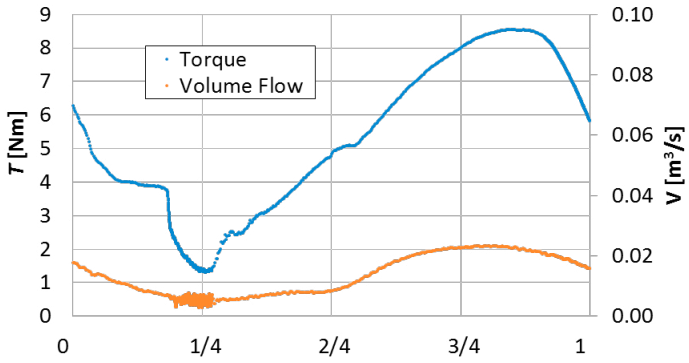

Fig. 8. Torque and volume flow at the inlet section as a function of normalized crankshaft angle with R134a

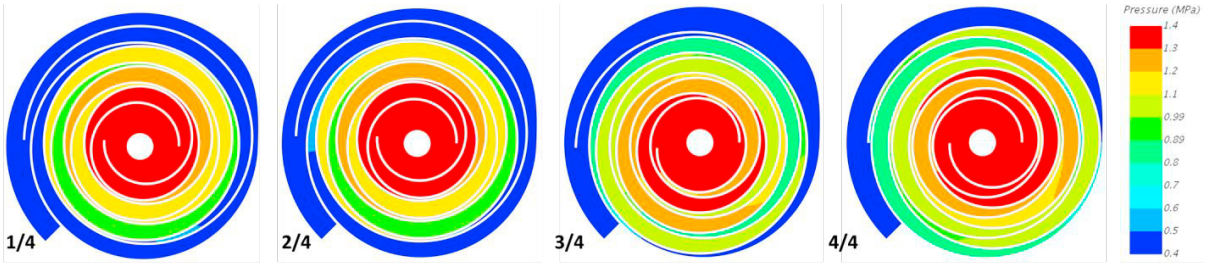

Fig. 9. Pressure plots inside the scroll, fluid: R134a

the issues that affect the scroll operation and the ORC system, such as vibrations or incomplete expansion of the fluid within the machine.

References

[1] Landelle A, Tauveron N, Haberschill P, Revellin R, Colasson, S. Performance Evaluation and Comparison of Experimental Organic Rankine Cycle Prototypes from Published Data. Appl Energy, art in press (2017).
[2] Song P, Wei M, Shi L, Danish SN, Ma C. A review of scroll expanders for organic Rankine cycle systems. Appl Therm Eng 2015;75:54-64.
[3] Lemort V, Quoilin S, Cuevas C, Lebrun J. Testing and modeling a scroll expander integrated into an Organic Rankine Cycle. Appl Therm Eng 2009;29:3094-3102.
[4] Lemort V, Declaye S, Quoilin S. Experimental characterization of a hermetic scroll expander for use in a micro-scale Rankine cycle. P I Mech Eng A-J Pow 2012;226:126-36.
[5] Declaye S, Quoilin S, Guillaume L, Lemort V. Experimental study on an open-drive scroll expander integrated into an ORC (Organic Rankine Cycle) system with R245fa as working fluid. Energy 2013;55:173-83.
[6] Wang H, Peterson RB, Herron T. Experimental performance of a compliant scroll expander for an organic Rankine cycle. P I Mech Eng A-J Pow 2009;223:863-72.
[7] Harada KJ, "Development of a Small Scale Scroll Expander", Master of Science Thesis in Mechanical Engineering, Oregon State University, Oregon, US; 2010.
[8] Bracco R, Clemente S, Micheli D, Reini M. Experimental tests and modelization of a domestic-scale ORC (Organic Rankine Cycle). Energy 2013;58:107-16.
[9] Chang JC, Chang CW, Hung TC, Lin JR, Huang KC. Experimental study and CFD approach for scroll type expander used in low-temperature organic Rankine cycle. Appl Therm Eng 2014;73:1444-52.
[10] Castilla R, Gamez-Montero PJ, Ertürk N, Vernet A, Coussirat M, Codina E. Numerical simulation of turbulent flow in the suction chamber of a gearpump using deforming mesh and mesh replacement. Int. J. Mech. Sci. 2010;52:1334-42.
[11] Del Campo D, Castilla R, Raush GA, Gamez-Montero PJ, Codina E. Numerical Analysis of External Gear Pumps Including Cavitation. J Fluids Eng 2012;134:081105.
[12] Ziviani D, Suman A, Lecompt S, De Paepe M, van den Broek M, Spina PR, Pinelli M, Venturini M, Beyene A. Comparison of a Single-Screw and a Scroll Expander under Part-Load Conditions for Low-Grade Heat Recovery ORC Systems. Proc. of 6th International Conference on Applied Energy 2014.
[13] Bagci E. Reverse engineering applications for recovery of broken or worn parts and re-manufacturing: Three case studies. Adv Eng Software 2009;40:407-18.
[14] Gameros A, De Chiffre L, Siller HR, Hiller J, Genta G. A reverse engineering methodology for nickel alloy turbine blades with internal features. CIRP J Manuf Sci Technol 2015;9:116-24.
[15] Morini M, Pavan C, Pinelli M, Romito E, Suman A. Analysis of a scroll machine for micro ORC applications by means of a RE/CFD methodology. Appl Therm Eng 2015;80:132-40.
[16] Steger JL, Benek JA. On the use of composite grid schemes in computational aerodynamics. Comput. Methods Appl. Mech. Eng. 1987;64:301–20.
[17] Togashi F, Nakahashi K, Ito Y, Iwamiya T, Shimbo Y. Flow Simulation of NAL Experimental Supersonic Airplane/Booster Separation Using Overset Unstructured Grids. Comput. Fluid, 2001;30:673-88.
[18] Schreck E, Perić M. Overset Grids in STAR-CCM+: Methodology, Applications and Future Developments. STAR Japanese Conference 2012.
[19] Ansys, Inc., 2013, "ANSYS Fluent Theory Guide, Release 15.0".
[20] Blazek J. Computational Fluid Dynamics: Principles and Applications, 2nd ed. Amsterdam: Elsevier; 2005.
[21] Suman A, Buratto C, Aldi N, Pinelli M, Spina PR, Morini M. A Comparison Between Two Different CFD Approaches of a Real Scroll Expander for Micro-ORC Applications. Proc. of the 3rd International Seminar on ORC Power Systems 2015.
[22] Ancona MA, Bianchi M, Branchini L, De Pascale A, Melino F, Orlandini V, Ottaviano S, Peretto A, Pinelli M, Spina PR, Suman A. A Micro-ORC Energy System: Preliminary Performance and Test Bench Development. Energy Procedia 2016;101:814-21.